View metadata, citation and similar papers at core.ac.uk
brought to you by CORE
provided by Digital.CSIC

Downwelling and dominance of autochthonous dinoflagellates in the NW Iberian margin: the example of the Ría de Vigo

B.G. Crespo*, F.G. Figueiras, P. Porras, I.G. Teixeira

Instituto de Investigacións Mariñas, CSIC, Eduardo Cabello 6, 36208 Vigo, Spain

* CORRESPONDING AUTHOR. Tel.: +34986 231930; fax: +34986 292762

E-mail address: bibiana@iim.csic.es (B.G. Crespo)

Abstract

Dinoflagellate blooms in coastal upwelling systems are restricted to times and places with reduced exchange and mixing. The Rías Baixas of Galicia are four bays in the NW Iberian upwelling with these characteristics where harmful algal blooms (HABs) of dinoflagellates are common. These blooms are especially recurrent at the end of the upwelling season, when autumn downwelling amplifies accumulation and retention through the development of a convergence front in the interior of rías. Because oceanic water enters the rías during downwelling, it has been hypothesised that dinoflagellate blooms originate by the advection and subsequent accumulation of allochthonous populations. To examine this possibility, we studied the microplankton succession in relation to hydrographic variability in the Ría de Vigo (one of these four bays) along an annual cycle making use of a high sampling frequency. The results indicated that upwelling lasted from May to August, with downwelling prevailing in winter. Microplankton during upwelling, although dominated by diatoms, evidenced a progressive increase in the importance of dinoflagellates, which achieved maximum abundance at the end of the upwelling season. Thus, diatoms characterised the spring bloom, while diatoms and autochthonous dinoflagellates composed the autumn bloom. Diatoms dominated during the first moments of the autumn downwelling and dinoflagellates were more abundant later, after stronger downwelling removed diatoms from the water column. Since the dinoflagellates selected by downwelling belonged to the local community, it is concluded that advection of alien populations is not required to explain these autumn blooms.

Keywords: dinoflagellate dominance, downwelling, NW Iberian upwelling, reversal circulation, Ría de Vigo

1. Introduction

Diatom dominance in well-mixed and nutrient replete waters and a major contribution of dinoflagellates in stratified and relatively nutrient poor water columns characterise the microplankton composition in coastal upwelling systems (Margalef, 1978a; Margalef et al., 1979; Smith et al., 1983). Thus, the microplankton succession progresses from diatom supremacy in spring to a higher importance of dinoflagellates in late summer-early fall (Margalef, 1958; Figueiras and Ríos, 1993). The distribution of microplankton assemblages also shows a distinctive spatial segregation typified by high diatom abundance near upwelling centres and a greater importance of dinoflagellates further offshore (Margalef, 1978b); a structure that frequently expands and contracts in response to upwelling-donwelling cycles (Margalef, 1978b; Tilstone et al., 1994). Although dinoflagellates can take advantage over diatoms in stratified water columns due to their ability to perform diel vertical migrations (Eppley and Harrison, 1975; Cullen, 1985; Cullen et al., 1985; Figueiras and Fraga, 1990; Fraga et al., 1992), blooms in coastal upwelling systems are mainly composed of diatoms, since those of dinoflagellates usually require physical processes leading to their accumulation. However, as some dinoflagellates are among the most noxious species causing harmful algal blooms (HABs) in coastal upwelling systems (Smayda, 1997), research on the oceanographic and biological processes ultimately responsible for their proliferation has been and still is a matter of continuous interest (GEOHAB, 2005). Accumulation and retention favoured by the vertical swimming capability of dinoflagellates have been repeatedly mentioned as the key factors promoting blooms of these species not only in coastal upwelling systems (Blasco, 1977; Pitcher et al., 1998), but also in bays (Tyler and Seliger, 1981; Anderson and Stolzenbach, 1985), estuaries (Chang and Carpenter, 1985) and in tidal fronts (Pingree et al., 1975). Advection of initial populations prior to

their accumulation in downwelling convergences is also occasionally necessary (e.g. Tyler and Seliger, 1981).

Blooms of dinoflagellates, often harmful, are relatively frequent in the Rías Baixas of Galicia, four bays on the NW Iberian peninsula (Fig. 1a) where seasonal upwelling-downwelling is one of the main oceanographic features (Blanton et al., 1984; Figueiras et al., 2002). The study of these blooms (e.g. Margalef, 1956; Fraga et al., 1988, 1990; Figueiras et al., 1994, 1996; Fermín et al., 1996), especially recurrent at the end of the upwelling season (Figueiras and Ríos, 1993), has provided a coherent picture for the dynamics of these type of HABs in the region. Seasonal upwelling on the NW Iberian shelf occurs, on average, from March to September when northerly winds are dominant, whereas downwelling prevails during the rest of the year owing to the predominance of southerly and westerly winds (Figueiras et al., 2002). Coastal upwelling and downwelling greatly influence the circulation in the rías and, therefore, the exchange between rías and the adjacent shelf (Figueiras et al., 1994; Fermín et al., 1996; Álvarez-Salgado et al., 2000; Tilstone et al., 2000). Upwelling forces a two layer density-induced positive circulation in the rías, characterised by the outflow of surface water and the compensating inflow of upwelled water at the bottom (Fig. 2a). Transition to seasonal downwelling, which coincides with the rapid change to southerly winds, establishes a circulation during which surface coastal water enters the rías to develop a downwelling front at the location where it meets the inner waters with higher continental influence (Fig. 2b). During this reverse circulation, the outflow towards the ocean in the outer circulation cell takes place at the bottom layer, while the inner cell maintains a positive circulation forced by runoff. The reverse circulation also modifies the distribution of microplankton assemblages along the rías and in the nearest shelf that, under upwelling conditions, is characterised by the dominance of diatoms in the

inner waters and a higher importance of dinoflagellates towards the shelf (Tistone et al., 1994). Downwelling causes the advection of dinoflagellates to the interior of the rías and promotes their accumulation in the downwelling front (Fraga et al., 1988; Figueiras et al., 1994; Fermín et al., 1996). This accumulation occurs because the vertical swimming capability of dinoflagellates allows them to compensate the downward velocity generated in this convergence (Figueiras et al., 1995). Diatoms, unable to counteract the downward velocity, are displaced down in the water column and then exported towards the shelf by the bottom outflow (Figueiras et al., 1994, 1996). Regardless of the selection of dinoflagellates by downwelling, the actual development into a bloom also needs the appropriate nutrient supply, which takes place by the return of moderate rather than strong upwelling conditions (Fermín et al., 1996; Figueiras et al., 1996), since strong upwelling enhances the positive circulation and favours diatom growth. High runoff, another nutrient source for the surface layer, also enhances the positive circulation and, hence, the displacement of the downwelling front towards the shelf. Therefore, the two processes, strong upwelling and runoff, tend to disperse dinoflagellates into the shelf waters.

Although selection of dinoflagellates by downwelling is generally accepted as the first necessary step for HABs development in the Rías Baixas during late summer, the source of the initial population is an issue that remains to be elucidated. Hypotheses maintaining both local (Figueiras et al., 1994; Fermín et al., 1996) and foreign origin (Fraga et al., 1988; Sordo et al., 2001) exist. The coincidence in time of the autumn upwelling-downwelling transition with the onset of a large-scale poleward current on the shelf (Frouin et al., 1990; Pingree et al., 1999; Álvarez-Salgado et al., 2003) has led to the suggestion that initial populations could be advected to the rías from the ocean (Fraga et al., 1988) or from the southernmost Portuguese coastal waters (Sordo et al.,

2001). As this controversy basically arises because studies on HABs dynamics in the region have been restricted to the short-time periods of HAB occurrence, the use of longer-term observations with high sampling frequency appears necessary to clarify the subject. We here present the results obtained from a twice-weekly sampling made over an annual cycle in the Ría de Vigo, when local microplankton succession ended in a short-lived dinoflagellate proliferation at the time of the autumn upwelling-donwelling transition.

2. Material and methods

A station situated in the mean channel (~45 m depth in low water) at the central part of the Ría de Vigo (Fig. 1b) was visited approximately twice a week from 20 January 1987 to 28 January 1988. Seawater samples from the surface and bottom (40 m) were collected with 5 litre Niskin bottles fitted with reversing thermometers. Temperature, salinity, nutrient concentration (nitrate, silicate, phosphate and ammonium), chlorophyll concentration and microplankton abundance were determined for each sampling and depth. These data were supplemented with daily determinations of incoming solar radiation, runoff in the drainage basin and along-shore and cross-shore Ekman transport components.

2. 1. Meteorology

Incoming solar radiation (Qs, cal cm^{-2} d^{-1}) was calculated using the Mosby's formula (Dietrich et al. 1980). Runoff (Qr, m^3 s^{-1}) was estimated following the empirical equation proposed by Ríos et al. (1992), which uses rainfall and a retention coefficient of 0.75 for the 586 km^2 drainage basin of the Ría de Vigo.

The cross-shore (Q_x) and along-shore (Q_y) Ekman transport components ($m^3\ s^{-1}\ km^{-1}$) were calculated according to Wooster et al. (1976):

$$Q_{X,Y} = \frac{\rho_{air} C_D |V| V_{Y,X}}{\rho_{sw} f}$$

where ρ_{air} is the air density (1.22 kg m^{-3}), C_D is the empirical drag coefficient (1.3 x 10^{-3}, dimensionless) according to Hidy (1972), f is the Coriolis parameter (9.946 x 10^{-5} s^{-1}) at 43º latitude and ρ_{sw} is the seawater density (~1025 kg m^{-3}). $V_{Y,X}$ is the vector of the wind speed on the sea surface, with magnitude $|V|$, which were deduced from the surface pressure charts (3 times d^{-1}) at the latitude of Cape Finisterre (43 ºN). Ekman transports calculated at Cape Finisterre are considered representative of the general conditions for the whole northwest Iberian coast, including the Rías Baixas (Blanton et al., 1984; Lavin et al., 1991). To facilitate comparisons between the 2 transport components the sign of the cross-shore transport (Q_X), which is associated with upwelling-downwelling on the shelf and corresponds to North-South winds, was changed: i.e. positive values of -Qx indicate upwelling and hence transport towards the open sea. East-West winds, which cause along-shore transport on the shelf (Q_Y), however have a different influence on the ría circulation owing to its almost perpendicular orientation to the main coast line (Fig. 1). Easterly winds enhance the outflow of surface waters of the Ría towards the open ocean and, therefore, cause upwelling inside the Ría. In contrast, westerly winds promote the intrusion of coastal surface waters into the ría and favour downwelling (Fig. 2b).

2.2. Hydrography, nutrients and chlorophyll

Temperature was registered with the reversing thermometers attached to the Niskin bottles. Salinity was calculated following UNESCO (1985) from conductivity determinations made with an AUTOSAL 8400A. Nutrient concentrations were determined using auto-analysers according to Hansen and Grasshoff (1983), with some improvements (Mouriño and Fraga, 1985).

Chlorophyll *a* concentrations were determined by fluorometry after filtration of 100 ml seawater samples under low vacuum pressure through 25 mm Whatman GF/F filters. Filters were frozen at -20 ºC until pigments were extracted in 90% acetone for 24 h in the dark at 4 ºC. Readings were made with a Turner Designs fluorometer calibrated with pure chlorophyll *a* (Sigma Chemical Co.).

2.3. Microplankton

Microplankton samples preserved in Lugol's iodine were sedimented in composite sedimentation chambers. The sedimented volume (10-50 ml) depended on the chlorophyll concentration of the sample. The organisms were counted and identified to the species level, when possible, using an inverted microscope. Two transects at x400 and x250 were used to count the small species. The larger and usually less abundant species were counted from the whole slide at x100 magnification.

Principal component analysis (PCA) was used to reduce and simplify the information contained in the list of species abundance, to identify assemblages and to determine changes in species composition. The analysis was made with the correlation matrix of species abundances after they were transformed to log (X + 1), X representing the number of individuals per 50 ml. To remove, as much as possible, zero values from the

matrix without losing information, only those species present in at least 30% of the samples were included in the analysis. This provided a starting matrix of 51 species x 101 samples for the surface samples. The very scattered presence of some species and the generally low cell abundance precluded the use of PCA with bottom samples.

3. Results

3.1. Meteorology and thermohaline properties

The freshwater supplied to the Ría de Vigo (Fig. 3a) showed both seasonal and short-term variability (average Qr = 26 ± 23 $m^3 s^{-1}$). High runoff took place between autumn and spring (Qr = 38 ± 24 $m^3 s^{-1}$), with the maximum freshwater input in autumn when a value of 130 $m^3 s^{-1}$ was recorded on 18 October. Runoff was low (Qr = 10 ± 7 $m^3 s^{-1}$) from late spring to the end of summer, coinciding with maximum solar radiation (Fig. 3a).

Upwelling, mainly caused by northerly winds (Fig. 3b), persisted from May to the end of August with intercalated short relaxation and even downwelling events. This seasonal upwelling was delimited by two winter periods with frequent and strong downwelling events. The autumn upwelling-downwelling transition firstly occurred through a relaxation in the second half of September (Fig. 3b) with weak southerly winds (mean –Qx = - 216 $m^3 s^{-1} km^{-1}$) that was quickly followed by a strong downwelling in October caused by westerly winds (Fig. 3c). Downwelling was particularly strong on 16-17 October (Qy < - 4000 $m^3 s^{-1} km^{-1}$) and coincided with the highest runoff (Fig. 3a). Downwelling in general and westerly winds (negative values of Qy) in particular were related to rainfall (Qy *vs* Qr, r = -0.51, P < 0.001, n = 374).

Seawater temperature (Fig. 3d) in the surface layer followed a seasonal variation that was partially correlated with solar radiation (r = 0.50, P < 0.001, n = 101). By

contrast, temperature in the bottom layer did not show any clear seasonal variation. Temperature in the bottom layer was rather constant (13.1 ± 0.4 ºC) from the beginning of the observations (January 1987) to the end of September, when it suddenly started to increase up to the values recorded in the surface layer: ~18 ºC on 8 October (Fig. 3c)

Variability in salinity was considerably higher in the surface than in the bottom layer (Fig. 3e). Because surface salinity was negatively correlated with runoff ($r = -0.66$, $P < 0.001$, $n = 101$), the highest differences in salinity between the two layers occurred during downwelling periods, when rainfall was more important. Thus, stratification of the water column was primarily caused by salinity during downwelling, while temperature was more important during the upwelling season (Fig. 3de).

3.2. Nutrients and chlorophyll

Except for the negative correlation found between nitrate and ammonium in the bottom layer, all the other nutrients were positively correlated among them, both in the surface and in the bottom (Table 1). Especially remarkable were the correlations between nitrate and silicate and between phosphate and ammonium in the surface and between silicate and phosphate in the bottom (Table 1). Higher nutrient concentrations in the surface than in the bottom (Figs. 4abcd) were only recorded during phases of high runoff (Fig. 3a), specifically in winter. Nitrate in the surface layer dropped to undetectable levels several times between March and October (Fig. 4a). In contrast, the other nutrients were never completely depleted (Fig. 4bcd).

Silicate concentration in the bottom layer increased continuously between May and September (Fig. 4b), as was confirmed by the correlation between Julian day and silicate concentration ($r = 0.76$, $P < 0.001$, $n = 41$). Phosphate levels in the bottom layer (Fig. 4c) also increased during the same period ($r = 0.67$, $P < 0.001$, $n = 41$). Although

in lesser extension, the same tendency was observed for nitrate (Fig. 4a, $r = 0.42$, $P < 0.01$, $n = 39$) and ammonium (Fig 4d, $r = 0.39$, $P < 0.05$, $n = 39$).

Regardless of the large variability evidenced by chlorophyll concentration in both layers, fortnightly averages (Fig. 4e) revealed two maxima in the surface that were separated by an intermediate summer period of lower but with steadily increasing concentrations. The spring maximum (~ 8 mg Chl m^{-3}) showed higher stability through time than the autumn maximum, in which the highest value of chlorophyll concentration (13.6 mg Chl m^{-3}), recorded at the beginning of the autumn upwelling-downwelling transition, was followed by low values (~ 2 mg Chl m^{-3}) after the strong downwelling of October. This seasonal variation was not observed in the bottom layer, where high chlorophyll values were found from early spring to middle summer and the autumn maximum was absent. Chlorophyll concentration during winter (~ 1 mg Chl m^{-3}) was similar in both layers.

3.3 Microplankton abundance

Microplankton in the surface layer (Fig. 5), which was essentially composed by diatoms (73%) and flagellates (24%), did not follow the chlorophyll pattern of maximum values in spring and autumn. Though microplankton abundance began to increase during early spring (late February) causing nutrient reduction (Fig. 4abcd), maximum abundance occurred at the beginning of the autumn upwelling-downwelling transition (end of September), when nutrients still remained low. Conspicuous temporal segregation existed at this time between diatoms and the other groups (dinoflagellates, flagellates and ciliates). Diatoms were more abundant at the end of September (Fig. 5a); whereas the other three groups reached their highest values later, during the stronger

downwelling conditions on the first week of October (Fig. 5bcd) coinciding with the chlorophyll maximum (Fig. 4e).

Starting from a relatively low winter abundance (~400 cells ml^{-1}) of diatoms (48%) and flagellates (47%), diatoms commenced to increase well in advance (late February) of the upwelling season (Fig. 3b) and prolonged their dominance (78%) until the beginning of the upwelling season in May (Figs. 5a, 3b). Chain-forming diatom species of medium and large size (e.g. Chaetoceros curvisetus, C. didymus, Asterionellopsis glacialis, Detonula pumila, Lauderia annulata, Guinardia striata, G. delicatula, Dactyliosolen fragilissimus) and small *Chaetoceros* (*C. socialis*) forming big spherical colonies composed this diatom community.

The microplankton community became more heterogeneous during the rest of the upwelling season (June-August) (Fig. 5bcd) due to the progressive appearance of dinoflagellates, flagellates and ciliates; diatoms accounted for 52%, flagellates 41% and dinoflagellates 6% of the total microplankton. Diatoms during this summer phase, which were of smaller size (e.g. small Chaetoceros spp., Skeletonema costatum, Leptocylindrus danicus and L. minimus) than those dominating in spring, coexisted with small flagellates, Cryptophyceae and the red tide flagellate Heterosigma akashiwo. Even though small Gymnodinium spp. were dominant within the dinoflagellate community, larger species (mainly Ceratium furca and C. fusus) were also noticeable in August. Dinoflagellates (Fig. 5b) and ciliates (Fig. 5d) also showed a conspicuous increase of abundance during the short downwelling events of June and August (Fig. 3b).

Diatoms, accounting for 85% of the total cell abundance, caused the extraordinary increase of microplankton abundance in September (Fig. 5a), which coincided with the upwelling relaxation that preceded the strong downwelling of October (Fig. 3bc). Later,

at the beginning of October, total microplankton abundance dropped to levels less than a half, when diatoms practically disappeared from the surface layer (1% of the total cell abundance) and dinoflagellates, flagellates and ciliates reached their highest abundances of the year (Fig. 5bcd). Ceratium fusus was the most abundant dinoflagellate species during this short period of time. At the end of October, once the strong downwelling had relaxed, microplankton abundance dropped even more, down to winter levels (~ 500 cells ml^{-1}), flagellates representing 85% and dinoflagellates 9% of the total cell abundance.

Following the short recovery of November (Fig. 5) caused by diatoms (Fig. 5a), microplankton abundance remained at low levels (~ 700 cells ml^{-1}) for the rest of the winter. In contrast to the previous winter period when diatoms and flagellates co-dominated, diatoms were now more abundant (70%) than flagellates (25%).

Total microplankton abundance in the bottom layer was considerably lower (Fig. 6) and, like in the surface layer, generally followed diatom abundance (Fig. 6a). The exception was during the autumn upwelling-downwelling transition with flagellates representing 75% of the total cell abundance. Previously, at the beginning of September, diatoms accounted for 80%.

3.4 Microplankton assemblages in the surface layer

Principal Component Analysis (PCA) extracted 2 components that explained 32% of the total variance in the original data set and allowed definition of the main microplankton assemblages present in the surface layer. Among all species or groups included in the analysis only 5 species (Eutreptiella sp., Torodinium robustum, Thalassionema nitzschioides, Coscinodiscus radiatus and Skeletonema costatum) showed negative loads with the first principal component PC1 (Table 2). Several large

dinoflagellates, including Ceratium furca and C. fusus, were the species with the highest positive loads with this component. The PC 1 scores increased continuously from negative to positive values between January and the beginning of October (Fig. 7a) ($r = 0.84$, $P < 0.001$, $n = 70$ between Julian day and scores of PC 1). Positive scores were maintained from the onset of the upwelling season in May to the first week of October when quickly jumped down to negative values that persisted until the end of the sampling period.

The dinoflagellate Ceratium fusus and the Raphidophycean Heterosigma akashiwo were the species with the highest positive loads (> 0.40) with the second component PC 2 (Table 2). Other dinoflagellates such as Heterocapsa niei, Prorocentrum micans, Protoperidinium divergens and Ceratium furca also had positive loads > 0.35. All the species with negative loads < -0.4 were diatoms, within which large species such as Chaetoceros spp., Asterionellopsis glacialis, Thalassiosira rotula and Detonula pumila predominated. Negative scores of PC 2 (Fig. 7b) persisted during the spring bloom between February and April, while positive and negative scores alternated during the upwelling season. Although positive scores of PC 2 were found in July and August and during winter, the highest positive values were achieved at the end of September and in October, during the autumn upwelling-downwelling transition.

4. Discussion

Although the study of microplankton dynamics in relation to physical processes in the highly variable environment of the Ría de Vigo ideally requires sampling programmes covering all the relevant spatial and temporal scales (e.g. Figueiras et al., 1994; Fermín et al., 1996; Tilstone et al., 2000), the use of the single station that we show here, where oceanic and continental influences are clearly discernible (Figueiras et

al., 1994, 2002), has proven to be a simple but helpful approach when the seasonal variability is the main concern (Nogueira et al., 1997, 2000; Nogueira and Figueiras, 2005). Therefore, strong seasonal signals, specifically those occurring in spring and autumn transitions, can be interpreted making use of the extensive knowledge gathered on circulation and microplankton distribution in the rías.

Despite short-term variability (Fig. 3bc), seasonality was an evident feature of the environmental conditions in the Ría de Vigo (Fig. 3), with downwelling dominating in winter and upwelling being more important in summer (Fig. 3bc). The driving force of the two-layered circulation in the inner cell (Fig. 2b) during winter was the high runoff (Fig. 3a), which also caused salinity stratification of the water column (Fig. 3e) and, therefore, was responsible for the formation of the two layers (Fig. 2). Under these circumstances, the relative strength of downwelling and runoff determines the position of the downwelling front (Fig. 2b) along the ría, with downwelling favouring an inner location and runoff forcing an outer position of the front (Álvarez-Salgado et al., 2000). The reversal circulation begins to affect the middle ría, where our station is located, when $-Qx/Qr < -7 \pm 2$. Contrarily, the formation of the two layers in summer was due to thermal stratification (Fig. 3d), when upwelling forced the circulation (Figueiras et al., 1994; Fermín et al., 1996; Álvarez-Salgado et al., 2000). The autumn upwelling-downwelling transition (end of September-beginning October, Fig. 3bcd) occurred, as frequently reported, through a downwelling event that brought warm surface water from the shelf to the ría interior (Figueiras et al., 1994, 2002; Álvarez-Salgado et al., 2000). This caused the thermal homogenisation of the water column (Fig. 3d), which took place through the rapid elevation of the temperature in the bottom layer up to the values recorded in the surface layer. Such homogenisation, without appreciable temperature changes in the surface layer could only be due to a strong downwelling that pushed the

warm surface water down to the bottom (Figueiras et al., 1994, 2002). Homogenisation by upwelling necessarily would have produced a significant decrease in the temperature of the surface layer through mixing with the cold upwelled water in the bottom. Additional evidence for the existence of reversal circulation in the middle ría during this autumn transition comes from the mean –Qx/Qr = 11 recorded between 15 September and 15 October.

Upwelling, which was practically the only nutrient source for the surface layer of the Ría de Vigo during summer, however did not cause persistent phytoplankton blooms. The reason for the absence of summer phytoplankton blooms was the positive circulation imposed by upwelling (Fig. 2a) that induced the export of material, and hence phytoplankton, from the ría towards the shelf. The two-layered circulation and, therefore, the export of phytoplankton was greatly favoured by the stratification of temperature (Fig. 3d) that allowed the efficient transmission between vertical (upwelling) and horizontal (export) velocities (Figueiras et al., 1994). While transported, a significant part of this material sinks to the bottom in the outermost part of the ría and in the nearest shelf where it experiences regeneration processes contributing to the progressive nutrient increase brought to the ría through the bottom layer by successive summer upwelling events (Fig. 4). This nutrient enrichment due to regeneration, which can represent up to 50% (nitrate) and 80% (silicate) of the total nutrient load supplied to the rías by the upwelled water at the end of the upwelling season in September (Alvarez-Salgado et al., 1997), fueled the continuous increase of chlorophyll concentration observed during the upwelling season (May-August, Fig. 4e).

The highest blooms took place during downwelling moments, before (spring) and after (autumn) the upwelling season (Figs. 3b, 4e). Spring and autumn phytoplankton blooms, which are recurrent in the Rías Baixas (Nogueira et al., 1997), occurred

because of the reversal circulation imposed by downwelling (Fig. 2b) that prevented exportation. The mechanism of formation and the phytoplankton composition of these two blooms were, however, substantially different. The spring bloom, mainly composed of large diatoms, developed inside the rías favoured by salinity stratification (Fig. 3e) and downwelling that blocked the export towards the shelf allowing phytoplankton accumulation. The high chlorophyll values (Fig. 4e) did not show correspondence with cell numbers (Fig 5) due to the large size of the diatoms that formed this bloom. On the contrary, the autumn bloom, which took place just after the upwelling period during which export was favoured, was caused by the advection towards the ría interior of microplankton populations previously exported towards the shelf. This interpretation, already suggested before (Figueiras et al., 1994, 1995, 1996; Tilstone et al., 1994; Fermín et al., 1996), is here supported by the succession of microplankton groups recorded in the surface layer during this relatively short-time period (Fig. 5). The accumulation of diatoms at the beginning of downwelling (end of September, Fig. 5a) was followed by the appearance of swimmers (dinoflagellates, flagellates and ciliates, Fig. 5bcd) in the first half of October, when downwelling began to be stronger (Fig. 3bc). Such sequence of events could only occur because downwelling, through the advection of surface water, transposed into a temporal scale in the ría interior the existing spatial segregation of microplankton along the ría, characterised by higher diatom dominance in the inner ría and a major importance of dinoflagellates in the outer ría (Tilstone et al., 1994; Figueiras et al., 1994, 1995). Dinoflagellates and flagellates (Figs. 5bc, 6bc) that remained in the water column during the first moments of downwelling (end of September-beginning October) due to their swimming capability (Fraga et al., 1989; Figueiras et al., 1995), however, were practically removed by the posterior stronger downwelling of middle October (Fig. 3c, $Qy < -2000$ m^3 s^{-1} k^{-1})

when downward velocities were presumably higher. Diatoms quickly disappeared during the first downwelling moments, not only from the surface (Fig. 5a) but also from the bottom layer (Fig. 6a), probably swept towards the ocean by the reversal circulation (Figueiras et al., 1994; Fermín et al., 1996).

According to the formation mechanism of this autumn bloom it could be hypothesised that dinoflagellates were foreign components of the local microplankton community that were advected to the ría by downwelling. However, the principal component analysis revealed that dinoflagellates were normal constituents of the microplankton community in the surface layer of the Ría de Vigo (PC 1 in Table 2), where the microplankton succession was characterised by the higher importance of dinoflagellates as summer progressed (Fig. 7a). The PCA also showed that some of these dinoflagellates (Ceratium fusus, Heterocapsa niei, Prorocentrum micans, and Ceratium furca) together with the raphidophyte Heterosigma akashiwo, were the species which were effectively selected by the autumn downwelling (PC 2 in Table 2, Fig. 7b).

5. Conclusion

We conclude, in agreement with several previous researchers, that downwelling is the oceanographic process that triggers dinoflagellate dominance in the Ría Baixas in autumn. Although advection of foreign populations can not be totally disregarded, we found that advection of alien dinoflagellate populations is not a requisite to explain this sudden dominance, which might be well understood through the positive selection of autochthonous populations. Despite initial selection by moderate downwelling, further stronger downwelling removes these dinoflagellate populations from the water column, precluding their later development into bloom conditions. This points to the very narrow environmental window that autumn HABs of dinoflagellates require for their

appearance in the region, where suitable downwelling for initiation adds to the succeeding weak upwelling and low runoff needed for their later development.

Acknowledgements

We thank the members of the Oceanography team at the Instituto de Investigacións Mariñas, Vigo, who participated in the sampling and analysis of nutrients and hydrographic variables. Financial support for this work came from the EU HABILE project (EVK3-CT-2001-00063). B.G.C. was funded by a predoctoral I3P fellowship of CSIC-European Social Foundation and I.G.T. by a FCT (Portuguese Foundation for Science and Technology) doctoral fellowship. This is a contribution to the GEOHAB Core Research Project – HABs in Upwelling Systems.

References

Álvarez-Salgado, X.A., Castro. C.G., Pérez. F.F., Fraga, F., 1997. Nutrient mineralization patterns in shelf waters of the Western Iberian upwelling. Cont. Shelf Res. 17, 1247-1270.

Álvarez-Salgado, X.A., Figueiras, F.G., Pérez, F.F., Groom, S., Nogueira, E., Borges, A.V., Chou, L., Castro, C.G., Moncoiffé, G., Ríos, A.F., Miller, A.E.J., Frankignoulle, M., Savidge, G., Wollast, R., 2003. The Portugal Coastal Counter Current off NW Spain: new insights on its biogeochemical variability. Prog. Oceanogr. 56, 281-321.

Álvarez-Salgado, X.A., Gago, J., Míguez, B.M., Gilcoto, M., Pérez. F.F., 2000. Surface waters of the NW Iberian margin: Upwelling on the shelf versus outwelling of upwelled waters from the Rías Baixas. Est. Coast. Shelf Sci. 51, 821-837.

Anderson, D.M., Stolzenbach, K.D., 1985. Selective retention of two dinoflagellates in a well-mixed estuarine embayment: the importance of diel vertical migration and surface avoidance. Mar. Ecol. Prog. Ser. 25, 39-50.

Blanton, J.O., Atkinson, L.P., Fernández de Castillejo, F., Lavín, A., 1984. Coastal upwelling off the Rías Bajas, Galicia, Northwest Spain, I: Hydrography studies. Rapp. p.-v. Reun. Cons. Int. Explor. Mer. 183, 79-90.

Blasco, D., 1977. Red tide in the upwelling region of Baja California. Limnol. Oceanogr. 22, 255-263.

Chang, J., Carpenter, E.J., 1985. Blooms of the dinoflagellate Gyrodinium aureolum in a Long Island estuary: Box model analysis of bloom maintenance. Mar. Biol. 89, 83-93.

Cullen. J.J., 1985. Diel vertical migration by dinoflagellates: roles of carbohydrate metabolism and behavioural flexibility. In: Rankin, M.A. (Ed.), Migration: mechanisms and adaptative significance. Univ. Texas Mar. Sci. Inst. Suppl. 27, 135-152.

Cullen, J.J., Zhu, M., Davis, R.F., Pierson, D. C., 1985. Vertical migration, carbohydrate synthesis, and nocturnal nitrate uptake during growth of Heterocapsa niei in a laboratory water column. In: Anderson, D.M., White, A.W., Baden, D.G. (Eds.), Toxic dinoflagellates. Elsevier, New York, pp. 189-194.

Dietrich, G., Kalle, K., Kraus, W., Siedler, G., 1980. General oceanography. An introduction, 2nd edn. John Wiley and Sons, New York

Eppley, R.W., Harrison, W. O., 1975. Physiological ecology of Gonyaulax polyedra, a red water dinoflagellate of Southern California. In: LoCicero, V. (Ed.), Toxic Dinoflagellate Blooms. Massachusetts Science Technological Foundation, Wakefield, pp. 11-22.

Fermín, E.G., Figueiras, F.G., Arbones, B., Villarino, M. L., 1996. Short-time scale development of a Gymnodinium catenatum population in the Ría de Vigo (NW Spain). J. Phycol. 32, 212-221.

Figueiras, F.G., Fraga, F., 1990. Vertical nutrient transport during proliferation of Gymnodinium catenatum Graham in the Ría de Vigo, Northwest Spain. In: Granéli, E., Sundström, B., Edler, L., Anderson, D. M. (Eds.), Toxic marine phytoplankton, Elsevier, New York, pp. 144-148.

Figueiras, F.G., Gómez, E., Nogueira, E., Villarino, M. L., 1996. Selection of Gymnodinium catenatum under downwelling conditions in the Ría de Vigo. In: Yasumoto, T., Oshima, Y., Fukuyo, Y. (Eds.), Harmful and Toxic Algal Blooms. Intergovernmental Oceanographic Commission of UNESCO, Paris, pp. 215-218.

Figueiras, F.G., Jones, K.J., Mosquera, A.M., Álvarez-Salgado, X.A., Edwards, A., MacDougall, N., 1994. Red tide assemblage formation in an estuarine upwelling ecosystem: Ria de Vigo. J. Plankton Res. 16, 857-878.

Figueiras, F.G., Labarta, U., Fernández Reiriz, M.J., 2002. Coastal upwelling, primary production and mussel growth in the Rías Baixas of Galicia. Hydrobiologia 484, 121-131.

Figueiras, F.G., Ríos, A.F., 1993. Phytoplankton succession, red tides and the hydrographic regime in the Rías Bajas of Galicia. In: Smayda, T.J., Shimizu, Y. (Eds.), Toxic phytoplankton blooms in the Sea. Elsevier, New York, pp. 239-244.

Figueiras, F.G., Wyatt, T., Álvarez-Salgado, X.A., Jenkinson, I., 1995. Advection, diffusion, and patch development of red tide organisms in the Rías Baixas. In: Lassus, P., Arzul, G., Erard, E., Gentin, P., Marcaillou, C. (Eds.), Harmful Marine Algal Blooms. Technique et Documentacion-Lavoisier, Intercept Ltd, pp. 579-584.

Fraga, F., Pérez, F.F., Figueiras, F.G., Ríos, A.F., 1992. Stoichiometric variations of N, P, C and O_2 during a Gymnodinium catenatum red tide and their interpretation. Mar. Ecol. Prog. Ser. 87, 123-134.

Fraga, S., Anderson, D.M., Bravo, I., Reguera, B., Steidinger, K.A., Yentsch, C.M., 1988. Influence of upwelling relaxation on dinoflagellates and shellfish toxicity in Ria de Vigo, Spain. Est. Coast. Shelf Sci. 27, 349-361.

Fraga, S., Gallager, S.M., Anderson, D.M., 1989. Chain-forming dinoflagellates: an adaptation to red tides. In: Okaichi, T., Anderson, D.M., Nemoto, T. (Eds.), Red tides: biology, environmental science and toxicology, Elsevier, New York, pp. 281-284.

Fraga, S., Reguera, B., Bravo, I., 1990. Gymnodinium catenatum bloom formation in the Spanish rias. In: Granéli, E., Sundström, B., Edler, L., Anderson, D.M. (Eds.), Toxic marine phytoplankton, Elsevier, New York, pp. 149-154.

Frouin, R., Fiúza, A.F. G., Ambar, I., Boyd, T.J., 1990. Observations of a poleward surface current off the coasts of Portugal and Spain during winter. J. Geophys. Res. 95, 679-691.

GEOHAB, 2005. Global Ecology and Oceanography of Harmful Algal Blooms, GEOHAB Core research project: HABs in upwelling systems. In: Pitcher, G., Moita, J., Trainer, V., Kudela, R., Figueiras, P., Probyn, T. (Eds.), IOC and SCOR, Paris and Baltimore

Hansen, H.P., Grassshoff, K., 1983. Automated chemical analysis. In: Grasshoff, K., Ehrardt, M., Kremling, K. (Eds.), Methods of seawater analysis, Verlag Chemie, Weinheim, pp. 347-395.

Hidy, G.M., 1972. A view of recent air-sea interaction research. Bull. Am. Meteorol. Soc. 53, 1083-1102.

Lavín, A., Díaz del Río, G., Cabanas, J.M., Casas, G., 1991. Afloramiento en el noroeste de la Península Ibérica. Indices de afloramiento para el punto 43º N 11ºW: Período 1966-1989. Inf. Tec. Inst. Esp. Oceanog. 91, 1-40.

Margalef, R., 1956. Estructura y dinámica de la "purga de mar" en la Ría de Vigo. Inv. Pesq. 5, 113-134.

Margalef, R., 1958. Temporal succession and spatial heterogeneity in phytoplankton. In: Buzzati-Traverso, A.A. (Ed.), Perspectives in Marine Biology. University California Press, Berkeley, pp. 323-348.

Margalef, R., 1978a. Life-forms of phytoplankton as survival alternatives in an unstable environment. Oceanol. Acta 1, 493-509.

Margalef, R., 1978b. Phytoplankton communities in upwelling areas. The example of NW Africa. Oecologia Aquatica 3, 97-132.

Margalef, R., Estrada, M., Blasco, D., 1979. Functional morphology of organisms involved in red tides, as adapted to decaying turbulence. In: Taylor, D.L., Seliger, H. H. (Eds.), Toxic dinoflagellate blooms, Elsevier, New York, pp. 89-94.

Mouriño, C., Fraga, F., 1985. Determinación de nitratos en agua de mar. Inv. Pesq. 49, 81-96.

Nogueira, E., Figueiras, F.G., 2005. The microplankton succession in the Ría de Vigo revisited: species assemblages and the role of the weather-induced, hydrodynamic variability. J. Mar. Syst. 54, 139-155.

Nogueira, E., Ibanez, F., Figueiras, F.G., 2000. Effect of meteorological and hydrographic disturbances on the microplankton community structure in the Ría de Vigo (NW Spain). Mar. Ecol. Prog. Ser. 203, 23-45.

Nogueira, E., Pérez, F. F., Ríos, A.F., 1997. Seasonal patterns and long-term trends in an estuarine upwelling ecosystem (Ría de Vigo, NW Spain). Est. Coast. Shelf Sci. 44, 285-300.

Pingree, R.D., Pugh, P.R., Holligan, P.M., Forster, G.R., 1975. Summer phytoplankton blooms and red tides along tidal fronts in the approaches to the English Channel. Nature 258, 672-677.

Pingree, R.D., Sinha, B., Griffiths, C.R., 1999. Seasonality of the European slope current (Goban Spur) and ocean margin exchange. Cont. Shelf Res. 19, 929-975.

Pitcher, G.C., Boyd, A.J., Horstman, D., Mitchell-Innes, B.A., 1998. Subsurface dinoflagellate populations, frontal blooms and the formation of red tide in the southern Benguela upwelling system. Mar. Ecol. Prog. Ser. 172, 253-264.

Ríos, A.F., Nombela, M., Pérez, F.F., Rosón, G., Fraga, F., 1992. Calculation of runoff to an estuary. Ría de Vigo. Sci. Mar. 56, 29-33.

Smayda, T.J., 1997, Harmful algal blooms: their ecophysiology and general relevance to phytoplankton blooms in the sea. Limnol. Oceanogr. 42, 1137-1153.

Smith, W.O., Heburn, G.W., Barber, R.T., O'Brien, J.J., 1983. Regulation of phytoplankton communities by physical processes in upwelling systems. J. Mar. Res. 41, 539-556.

Sordo, I., Barton, E.D., Cotos, J.M., Pazos, Y., 2001. An inshore poleward current in the NW of the Iberian Peninsula detected from satellite images, and its relation with G. catenatum and D. acuminata blooms in the Galician rias. Est. Coast. Shelf Sci. 53, 787-799.

Tilstone, G.H., Figueiras, F.G., Fraga, F., 1994. Upwelling-downwelling sequences in the generation of red tides in a coastal upwelling system. Mar. Ecol. Prog. Ser. 112, 241-253.

Tilstone, G.H., Míguez, B.M., Figueiras, F.G., Fermín, E.G., 2000. Diatom dynamics in a coastal ecosystem affected by upwelling: coupling between species succession, circulation and biogeochemical processes. Mar. Ecol. Prog. Ser. 205, 23-41.

Tyler, M.A., Seliger, H.H., 1981. Selection for a red tide organism: Physiological responses to the physical environment. Limnol. Oceanogr. 26, 310-324.

UNESCO, 1985. The international system of units (SI) in Oceanography. UNESCO Technical Papers in Marine Science 45

Wooster, W.S., Bakun, A., McLain, D.R., 1976. The seasonal upwelling cycle along the eastern boundary of the North Atlantic. J. Mar. Res. 34, 131-141.

Table 1. Correlation coefficients among nutrient concentrations in the surface and the bottom layers between 20 January 1987 and 28 January 1988 in the Ría de Vigo (n = 93; * P < 0.05; ** P < 0.01; *** P < 0.001).

Variables	Surface	Bottom
NO^-_3 – SiO_4H_4	0.91***	0.43***
NO^-_3 – HPO^{2-}_4	0.33**	0.51***
NO^-_3 – NH^+_4	0.43***	-0.21*
SiO_4H_4 – HPO^{2-}_4	0.37***	0.79***
SiO_4H_4 - NH^+_4	0.53***	0.53***
HPO^{2-}_4 - NH^+_4	0.82***	0.64***

Table 2. Correlation coefficients (loads) of the species and taxa selected for Principal Component Analysis (PCA) with the first 2 principal components. Species and taxa are ordered according to PC 1. The higher positive and negative loads for PC 2 are in bold type. The species were grouped as diatoms (Diat), dinoflagellates (Dinof), flagellates other than dinoflagellates (Flag) and ciliates (Cil).

Group	Taxon	PC 1	PC 2
Dinof	Ceratium furca	0.795	**0.354**
Dinof	Protoperidinium divergens	0.740	**0.358**
Dinof	Scrippsiella trochoidea	0.733	0.143
Dinof	Dinophysis acuminata	0.727	0.011
Dinof	Ceratium fusas	0.722	**0.441**
Cil	Ciliates (other than choreotrich, 30-60 µm)	0.719	0.114
Flag	Unidentified small flagellates (<30µm)	0.679	-0.043
Dinof	Protoperidinium longipes	0.673	-0.078
Cil	Choreotrich ciliates A (medium, 30-60 µm)	0.623	0.063
Diat	Leptocylindrus danicus	0.615	-0.306
Dinof	Protoperidinium steinii	0.613	0.244
Dinof	Heterocapsa niei	0.587	**0.392**
Flag	Leucocryptos spp.	0.574	0.120
Dinof	Protoperidinium diabolus	0.560	-0.094
Dinof	Gymnodinium spp. (small, <30µm)	0.560	0.159
Flag	Heterosigma akashiwo	0.541	**0.397**
Flag	Cryptophyceae spp.	0.534	0.035
Dinof	Gymnodinium varians	0.483	-0.359
Dinof	Gyrodinium fusiforme	0.469	-0.389
Diat	Pseudo-nitzschia cf. seriata	0.468	**-0.597**
Cil	Strombidium strobilum	0.463	-0.088
Dinof	Amphidinium flagellans	0.451	-0.004
Cil	Choreotrich ciliates (small, <30 µm)	0.447	0.054
Dinof	Prorocentrum micans	0.361	**0.381**
Diat	Centric diatom spp. (small, <30 µm)	0.352	-0.023

Diat	Pleurosigma elongatum	0.339	**-0.457**
Dinof	Naked dinoflagellates (medium, 30-60 µm)	0.311	0.036
Diat	Dactyliosolen fragilissimus	0.302	**-0.525**
Cil	Choreotrich ciliates (large, >60 µm)	0.282	0.083
Cil	Mesodinium rubrum	0.265	0.143
Diat	Thalassiosira rotula	0.264	**-0.599**
Diat	Detonula pumila	0.253	**-0.653**
Cil	Choreotrich ciliates B (medium, 30-60µm)	0.246	-0.132
Diat	Guinardia delicatula	0.232	-0.293
Cil	Ciliates (other than choreotrich, <30 µm)	0.200	-0.388
Diat	Rhizosolenia setigera	0.165	**-0.612**
Dinof	Gymnodinium nanum	0.160	-0.033
Diat	Chaetoceros didymus	0.135	**-0.782**
Diat	Chaetoceros spp. (small)	0.132	-0.287
Diat	Nitzschia longissima	0.125	-0.018
Diat	Chaetoceros debilis	0.086	**-0.567**
Diat	Chaetoceros lorenzianus	0.079	**-0.535**
Diat	Pseudo-nitzschia cf. delicatissima	0.065	**-0.533**
Diat	Centric diatom spp. (medium, 30-60 µm)	0.039	0.317
Diat	Chaetoceros curvisetus	0.036	**-0.608**
Diat	Asterionellopsis glacialis	0.011	**-0.805**
Flag	Eutreptiella sp.	-0.030	-0.065
Dinof	Torodinium robustum	-0.098	0.129
Diat	Thalassionema nitzschioides	-0.203	-0.390
Diat	Coscinodiscus radiatus	-0.251	0.032
Diat	Skeletonema costatum	-0.386	-0.149

Figure captions

Fig. 1. Map showing (a) the location of the four Rías Baixas on the NW of the Iberian Peninsula, and (b) detail of the Ría the Vigo with the sampling station.

Fig. 2. Scheme representing the circulation of the rías during (a) upwelling and (b) downwelling. See text for details.

Fig. 3. Evolution of (a) runoff Qr and incoming solar radiation Qs, (b) cross-shore Ekman transport - Qx, (c) along-shore Ekman transport Qy, (d) temperature and (e) salinity in the surface and bottom layers during the sampling period. Dashed areas denote the upwelling season and the autumn downwelling transition. See text for details.

Fig. 4. Evolution of (a) nitrate, (b) silicate, (c) phosphate, (d) ammonium and (e) chlorophyll concentration in the surface and bottom layer. Values were fortnightly averaged (n = 4) to remove short-term variability.

Fig. 5. Evolution of total microplankton abundance (cells mL^{-1}) in the surface layer compared with that of (a) diatoms, (b) dinoflagellates, (c) flagellates other than dinoflagellates and (d) ciliates during the sampling period. Values were fortnightly averaged (n = 4) to remove short-term variability.

Fig. 6. Evolution of total microplankton abundance (cells mL^{-1}) in the bottom layer compared with that of (a) diatoms, (b) dinoflagellates, (c) flagellates other than dinoflagellates and (d) ciliates during the sampling period. Values were fortnightly averaged (n = 4) to remove short-term variability.

Fig. 7. Evolution of (a) PC 1 and (b) PC 2 scores extracted by the principal component analysis of microplankton species abundance. Dashed areas denote the upwelling season and the autumn downwelling transition.

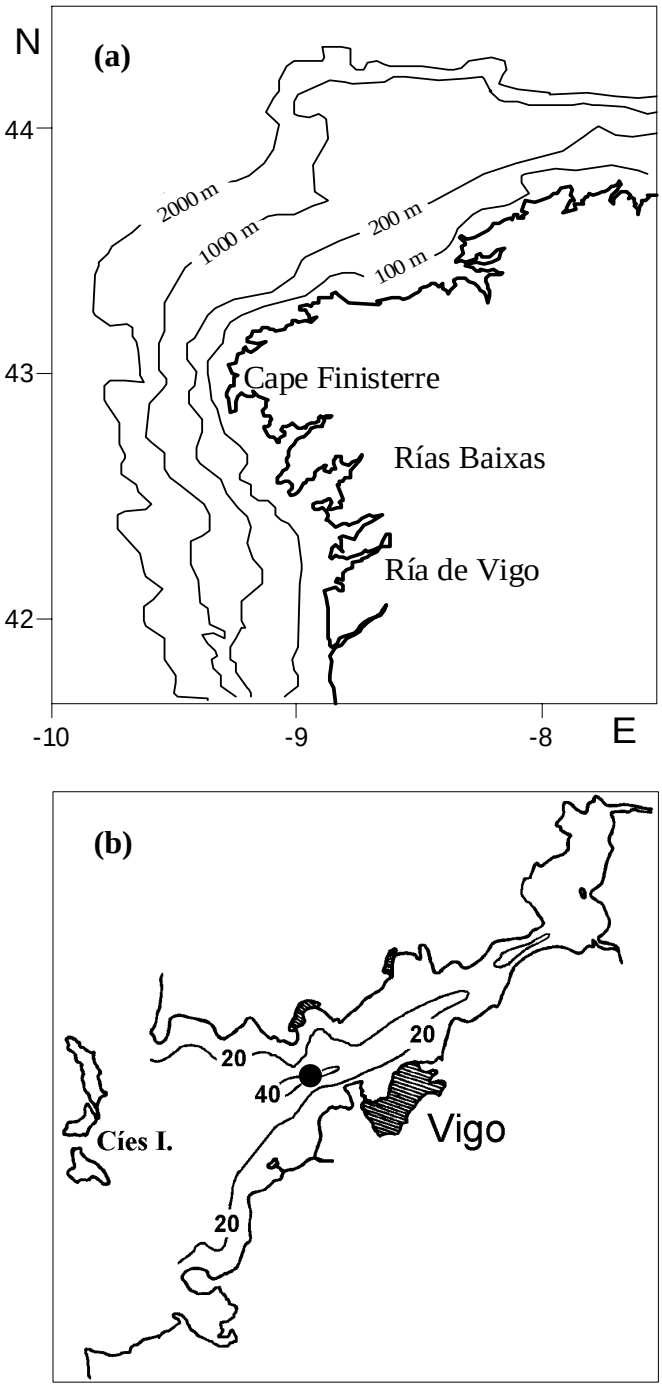

Fig. 1
Crespo et al.

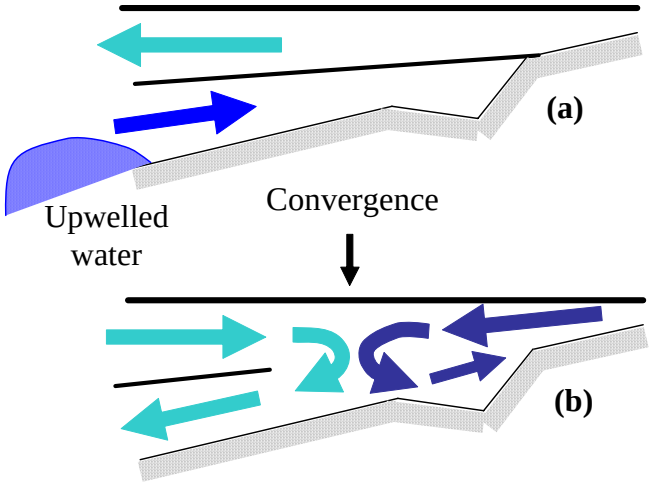

Fig. 2
Crespo et al.

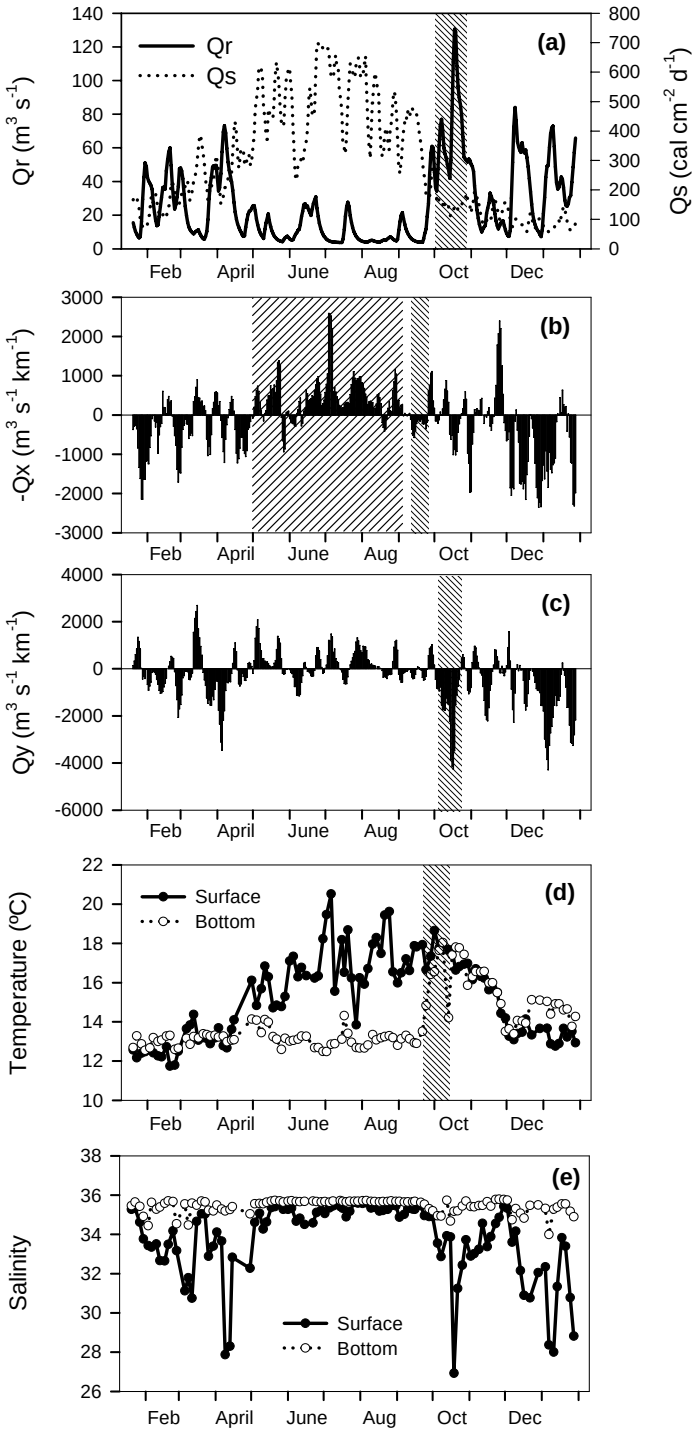

Fig. 3
Crespo et al.

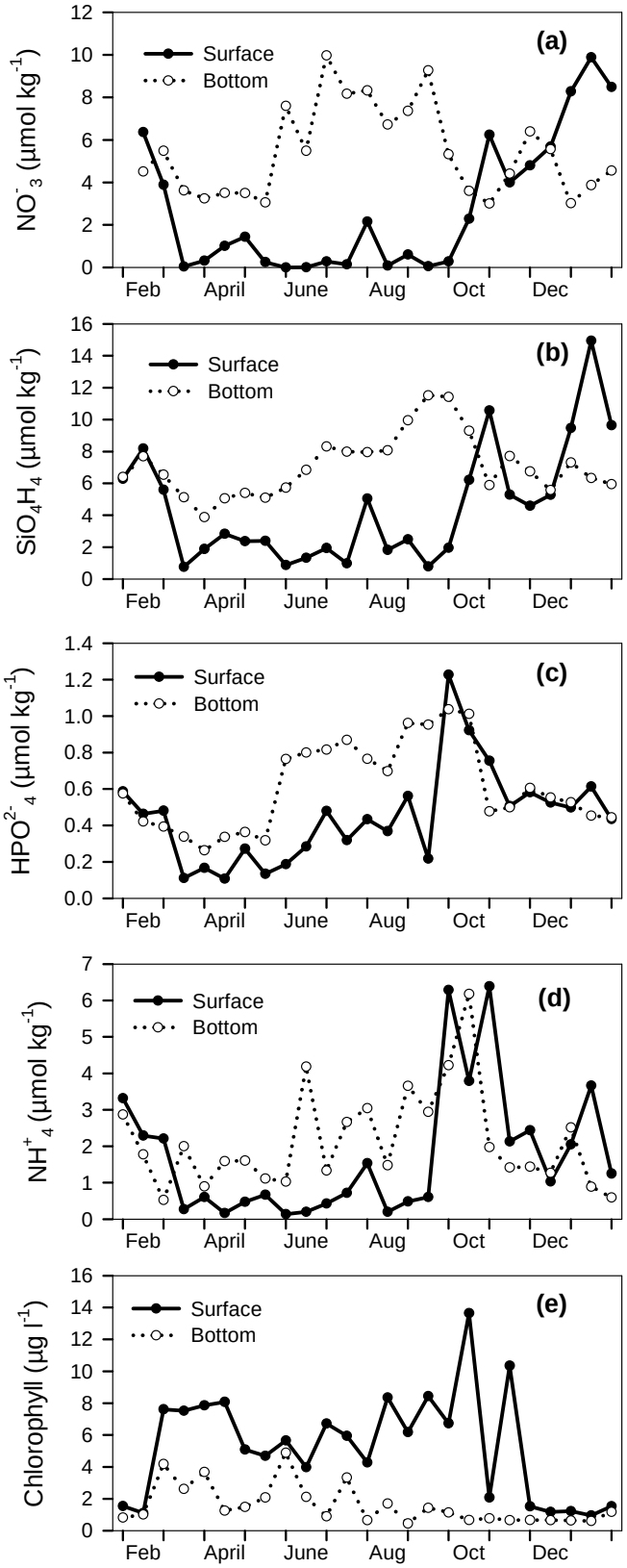

Fig. 4
Crespo et al.

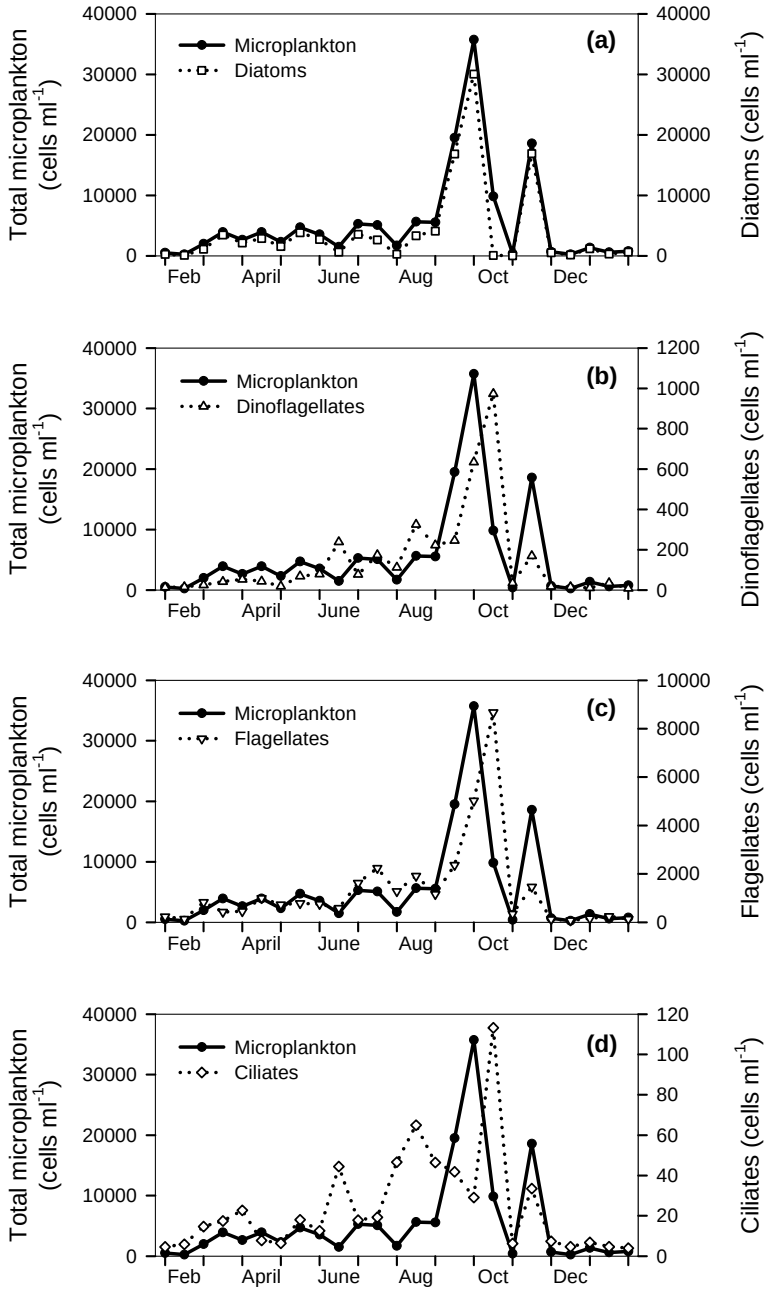

Fig. 5
Crespo et al.

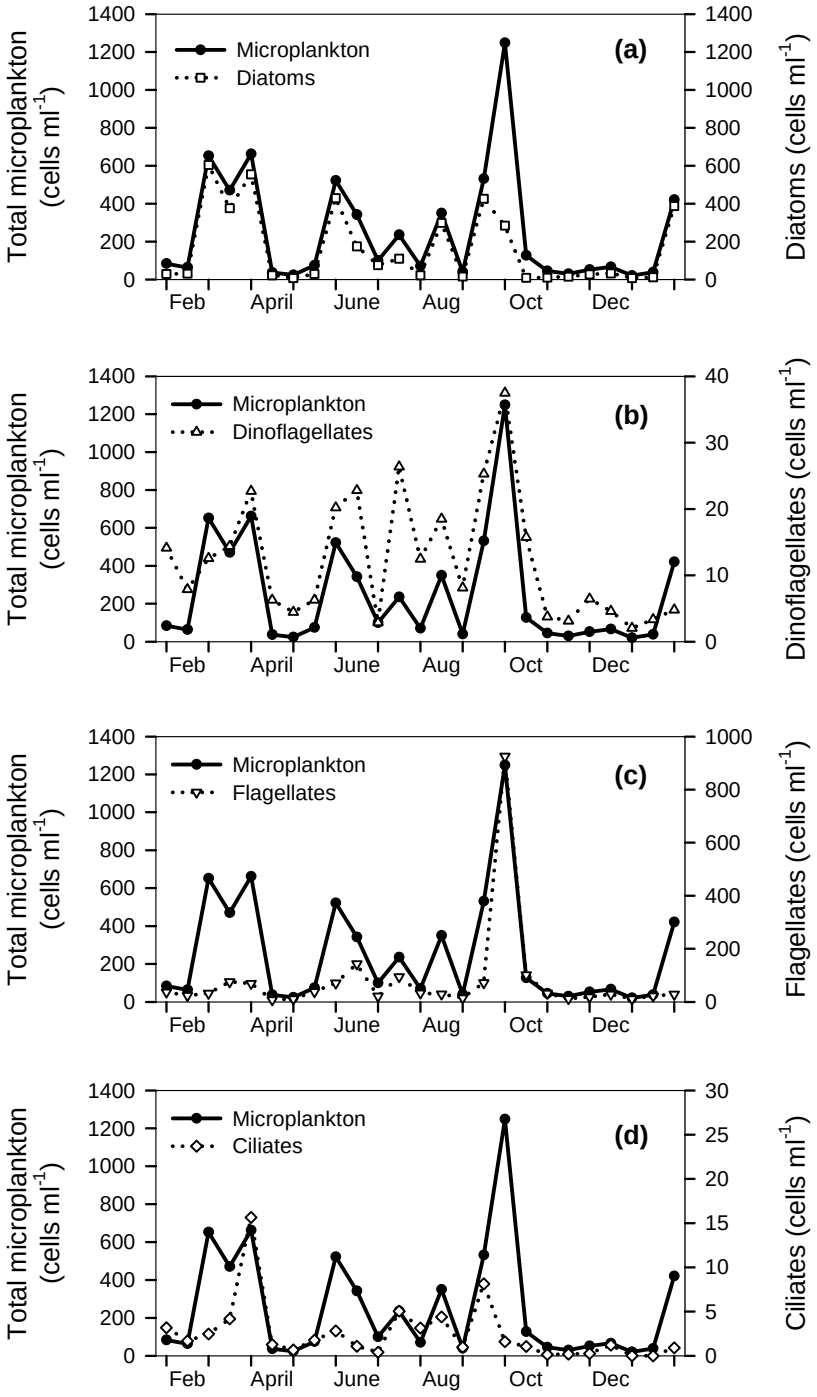

Fig. 6
Crespo et al.

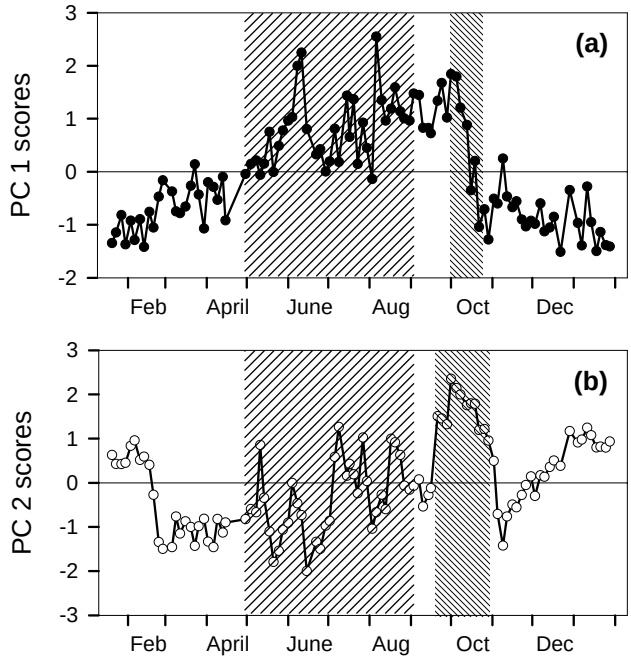

Fig. 7
Crespo et al.